



Electrochemical behavior and electrolytic preparation of lead in eutectic NaCl–KCl melts

Zeng-li ZHU¹, Huan LIU^{1,2}, Jie-shuang-yang CHEN¹, Hui KONG^{1,3}, Liang XU¹, Zhong-sheng HUA^{1,3}, Zhuo ZHAO¹

1. School of Metallurgical Engineering, Anhui University of Technology, Ma'anshan 243032, China;

2. Jinguan Copper Branch, Tongling Nonferrous Metals Group Holding Co., Ltd., Tongling 244000, China;

3. Anhui Provincial Key Laboratory of Metallurgical Engineering & Resources Recycling,
Anhui University of Technology, Ma'anshan 243002, China

Received 15 January 2020; accepted 16 June 2020

Abstract: A novel molten salt extraction process consisting of chlorination roasting and molten salt electrolysis was proposed to develop a more efficient and environmental friendly technology for recovering lead from spent lead acid batteries (LABs). The feasibility of this process was firstly assessed based on thermodynamics fundamentals. The electrochemical behavior of Pb(II) on a tungsten electrode in the eutectic NaCl–KCl melts at 700 °C was then investigated in detail by transient electrochemical techniques. The results indicated that the reduction reaction of Pb(II) in NaCl–KCl melts was a one-step process exchanging two electrons, and it was determined to be a quasi-reversible diffusion-controlled process. Finally, potentiostatic electrolysis was carried out at –0.6 V (vs Ag/AgCl) in the NaCl–KCl–PbCl₂ melts, and the obtained cathodic product was identified as pure Pb by X-ray diffraction analysis. This investigation demonstrated that it is practically feasible to produce pure Pb metal by electrochemical reduction of PbCl₂ in eutectic NaCl–KCl melts, and has provided important fundamental for the further study on lead recovery from spent LABs via molten salt extraction process.

Key words: electrochemical behavior; Pb(II); reduction; spent lead acid batteries; eutectic NaCl–KCl melt

1 Introduction

Lead is now widely used in industrial batteries, automotive and nuclear shielding materials, and plays a broad and strategically important role in the industrial development and global economy [1,2]. Among its many applications, the lead acid batteries (LABs) used in automobiles and power back-ups have consumed 70% of global lead produced annually [3]. Due to the sharp increasing demand for LABs worldwide, the lead production and consumption have kept increasing continuously in recent decades.

The resources for lead production could be classified into two types: the primary and the secondary. In fact, the global primary lead production has been kept almost static from 1970, and secondary lead production from recycling process has become the major source of lead and gradually dominated the global lead market [4]. In the future, the growth of global lead production will be continuously contributed by secondary lead.

Currently, spent LABs are the main resource of secondary lead and account for more than 85% of total secondary lead production [1]. On the other hand, spent LABs should be disposed properly from an environmental point of view, due to the high

Foundation item: Project (gxyq2018012) supported by the Developing Program Foundation for the Excellent Youth Talents of Higher Education of Anhui Province, China; Project (SKF19-05) supported by Foundation of Anhui Province Key Laboratory of Metallurgical Engineering & Resources Recycling, China; Projects (51904003, U1703130) supported by the National Natural Science Foundation of China

Corresponding author: Zhong-sheng HUA; Tel: +86-555-2311571; E-mail: huazs83@163.com

DOI: 10.1016/S1003-6326(20)65402-4

toxicity of lead [5]. Therefore, efficient and sustainable recycling of spent LABs is particularly critical for the sustainable development of lead industry and environmental protection.

Two types of lead-containing materials in the LABs, lead grid and paste, can be separated out from spent batteries. Lead grid, in metallic form, can be readily recovered by low temperature smelting due to its relatively stable compositions and low melting temperature, while the battery paste is composed of PbSO_4 (~60 wt.%), PbO_2 (~28 wt.%), PbO (~9 wt.%) and Pb (~3 wt.%) [5–7]. The battery paste is traditionally treated with pyrometallurgical technology at a high temperature above 1000 °C, either direct smelting or indirect smelting [1,5]. Although the smelting process has gained great progress in environmental protection and energy efficiency [8], the uncontrolled emission of lead-containing particulates and SO_2 gas still poses huge threat to the human and environment [9]. Compared with pyrometallurgical route, electro-hydrometallurgical technology is considered as an eco-friendly alternative due to its low operation temperature, less fine dust emission and high flexibility. However, it is less economically competitive with both significant capital investment and relatively high operating cost [4]. Additionally, the toxicity and severe corrosivity of HBF_4 and H_2SiF_6 used in dissolution and electrowinning processes are more likely to cause health risks and equipment corrosion. Consequently, developing a more efficient and environmentally-friendly technology for spent LABs recycling appears to be particularly important.

Chlorination metallurgy is a fairly effective and highly selective technique for nonferrous metals extraction by taking advantages of the low melting point and high volatility of metal chlorides, and the distinct differences in the formation of various metal chlorides [10–13]. The Pb-bearing phases in spent LABs can be readily converted to PbCl_2 by chlorination roasting at a relatively low temperature [1,14]. Subsequently, the separated PbCl_2 can be directly processed by electrolysis for metallic lead production, as molten salt electrolysis is an effective approach regarding the extraction of both base metals and reactive metals [15–17]. This molten salt extraction process is considered to be

quite promising for metal values recovery due to its environmental friendliness [15,18]. To practically facilitate the development of the proposed recycling technology, the electrochemical extraction of lead from molten salts should be studied first. Although the electrolysis of lead and its alloys in LiCl-KCl melts has been intensively investigated [2,19–21], the electrochemical reduction of Pb(II) in molten NaCl-KCl eutectic has not been fully clarified yet. In the present work, a systematic investigation on the electrochemical behavior of Pb(II) in eutectic NaCl-KCl melts was carried out using a series of transient electrochemical techniques. The results are of great importance to expand the fundamental knowledge of lead electrochemistry and lead recovery from spent LABs.

2 Experimental

NaCl and KCl (50.6:49.4, molar ratio) were selected as the supporting electrolyte in this work due to their good electrical conductivity, high thermal stability [22,23], and also commonly used industrial chlorinating reagents [24]. NaCl (>99.5% purity) and KCl (>99.5% purity) were firstly dried at 200 °C for more than 48 h and then melted in an alumina crucible in an electric furnace at 700 °C. Metallic impurities in the eutectic melts were removed by pre-electrolysis at -2.0 V (vs Ag/AgCl) for 3 h. Anhydrous PbCl_2 (analytical grade) was directly introduced into the melts as the resource of Pb(II) .

Cyclic voltammetry, square wave voltammetry, linear sweep voltammogram, chronopotentiometry and potentiostatic electrolysis were performed in a three-electrode cell using PARSTAT 2273 potentiostat (Ametek Group Co., American) with Powersuite software. A tungsten wire (99.99% purity) of 1.0 mm in diameter was used as the working electrode, and a spectral pure graphite rod of 6.0 mm in diameter was employed as the counter electrode. The reference electrode was a mullite tube containing a silver wire (99.99% purity) of 1.0 mm in diameter immersed in NaCl-KCl-AgCl (1 wt.%) melts. All potentials were referred to this Ag/AgCl couple in this study. All the experiments were conducted in a high-purity argon atmosphere. The metallic lead was produced by potentiostatic electrolysis at 700 °C. After electrolysis, the

cathodic products were mechanically separated from the melts, and then immersed in deionized water to remove the residual salts and further ultrasonically cleaned in ethanol (99.5% purity). The crystal structures of the sample were identified by X-ray diffraction (XRD, D8 Advance, Bruker Corporation) using a Cu K_{α} monochrome target.

3 Results and discussion

3.1 Process fundamentals

The proposed molten salt extraction process includes two consecutive steps, viz, (1) chlorination of the Pb-bearing substances in spent LABs by roasting with chlorides, and (2) electrolysis in the melts containing $PbCl_2$ to produce Pb metal. As previously discussed, spent LAB is the primary source for lead recovery at present and even in the future for a long period of time. During the chlorination roasting, solid chlorinating agents such as $CaCl_2$, $NaCl$, KCl and NH_4Cl are more favorable in application instead of Cl_2 or HCl in view of their severe corrosion to production facilities [24]. But importantly, the addition of $NaCl$, KCl or $CaCl_2$ is conducive for improving the physicochemical properties of the electrolyte, for example, increasing the conductivity, lowering the melting temperature and viscosity [25,26], and thus being beneficial for the subsequent electrolysis. For chlorination roasting, $CaCl_2$ is generally preferred in industrial application due to its low cost and relatively strong chlorinating ability [27]. The Gibbs free energy changes for potential chemical reactions of the Pb-bearing phases including $PbSO_4$, PbO_2 , PbO and Pb , chlorinated by $CaCl_2$ in the temperature range of 400–800 °C are given in Fig. 1. The changes in standard Gibbs free energy of the reactions, calculated by using the thermodynamic software HSC Chemistry 6, are fairly negative, indicating that all the Pb-bearing phases in spent LABs are easy to be chlorinated by roasting with $CaCl_2$. It is also worth noting that the practical feasibility has also been verified by LIU et al [28]. Similarly, the main component of the spent lead paste can also be chlorinated to $PbCl_2$ by roasting with $NaCl$, as seen in Fig. 1. However, it is obvious that the chlorinating ability of $NaCl$ is much weaker than that of $CaCl_2$. Herein, $CaCl_2$ is chosen for the chlorination roasting. Subsequently, high-purity $PbCl_2$ can be separated out via chloridizing

volatilization because of the low boiling point and high vapor pressure [28], and thus can be processed by molten salt electrolysis for Pb production.

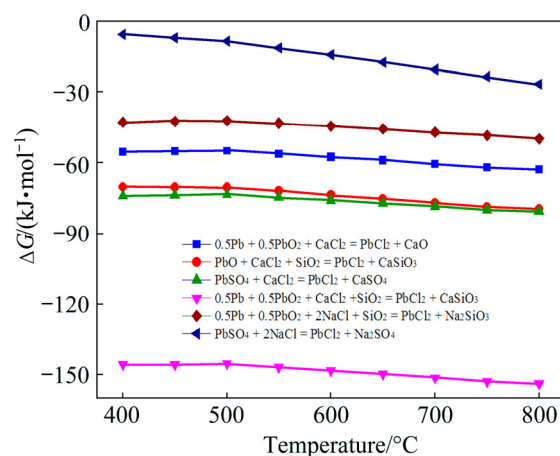


Fig. 1 Gibbs free energy changes of reactions between Pb-bearing phases and chlorinating reagents ($CaCl_2$ and $NaCl$) at 400–800 °C by using HSC Chemistry 6.0

Secondly, the deposition of Pb metal on the cathode should be favored electrochemically, and conversely, the reduction of other metal cations must be less prevalent for the electrowinning in the multicomponent melts. This is another prerequisite for the successful implementation of the molten salt extraction process. Thus, it is necessary to identify the decomposition voltages of several commonly used chlorides from the viewpoint of lead recovery. The theoretical decomposition voltages U (as presented in Fig. 2) for various metal chlorides were calculated by the following thermodynamic equation:

$$\Delta G^{\ominus} = -nFU \quad (1)$$

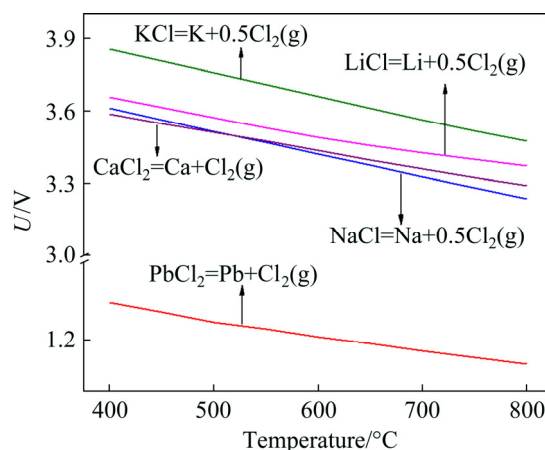


Fig. 2 Relationship between theoretical decomposition voltage of several metal chlorides and temperature

where ΔG^\ominus is the standard Gibbs free energy change of reaction (kJ/mol), n represents the number of transferred electrons for a given amount of reactant (mol), and F is Faraday constant (96485 C/mol). The data used for calculation are also obtained from HSC Chemistry 6 software. It is obvious that PbCl_2 has the lowest decomposition voltage compared with the other metal chlorides, which ensures the preferential selective deposition of Pb metal during the electrochemical process.

This novel salt extraction process based on chlorination roasting followed by molten salt electrolysis, for recycling lead from spent batteries is theoretically feasible and shows attractive environment-friendly features as follows: (1) no SO_2 emission because the elemental sulfur in PbSO_4 phase still exists in the form of sulfate after chlorination roasting, while the Cl_2 generated during electrolysis process can be absorbed by limewater to produce CaCl_2 ; (2) no adoption of corrosive and toxic materials such as HBF_4 and H_2SiF_6 which are required for lead dissolution and electrowinning in the electrochemical hydrometallurgical process. Moreover, molten salt electrolysis is an economically potential method for the recovery of metal values due to its high current density and productivity, and without limitation regarding H_2 evolution [15,29,30].

3.2 Electrochemical behavior of Pb(II)

To make direct electrodeposition of metal lead from molten salts practically feasible, the electrochemical behavior and electrolysis of Pb in eutectic NaCl–KCl melts were then investigated through a series of experiments. Figure 3 represents the cyclic voltammograms measured on a tungsten electrode in the NaCl–KCl eutectic melts before and after the addition of 0.65 wt.% PbCl_2 at 700 °C. The dotted curve in Fig. 3 presents the typical voltammogram of NaCl–KCl melts in the absence of PbCl_2 . The cathodic peak C1 appearing at approximately –2.0 V (vs Ag/AgCl) is attributed to the deposition of Na, and its corresponding anodic peak A1 in the reverse scan direction is associated with the dissolution of metallic Na. There are no additional reaction signals detected in the electrochemical window except for the redox peaks A1/C1, identifying the applicability of the melts for the investigation. The solid line displays the voltammogram after the addition of PbCl_2 . A new

cathodic peak C2 is observed, as clearly seen in the inset in Fig. 3, which should be ascribed to the one step reduction of Pb(II) to Pb(0) by Eq. (2):



In the positive-going scanning, the anodic signal A2 corresponds to the subsequent oxidation process of Pb(0) to Pb(II). In addition, the initial reduction potential of C2 is around –0.38 V (vs Ag/AgCl), which approximates to that detected by ZHANG et al [2] and HAN et al [21] in the electrochemical fabrication of Li–Pb alloys in LiCl–KCl melts. Noteworthy, apart from the signal couples C1/A1 and C2/A2, no other additional redox peaks present in cyclic voltammograms, and thus, it is highly probable that pure Pb metal can be deposited by direct electrochemical reduction of Pb(II) in NaCl–KCl melts.

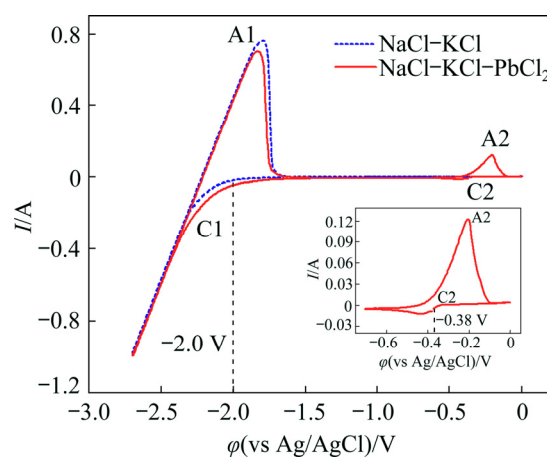


Fig. 3 Cyclic voltammograms of NaCl–KCl eutectic melts before (dotted line) and after (solid line) addition of 0.65 wt.% PbCl_2 on tungsten electrode with area of 0.322 cm² at 700 °C and scan rate of 0.1 V/s

Subsequently, square wave voltammetry was conducted to determine the number of exchange electrons in the cathodic process of Pb(II). Figure 4 displays the square wave voltammograms acquired on a tungsten electrode in molten NaCl–KCl– PbCl_2 at 700 °C and frequency of 30 Hz. There is an asymmetrical Gaussian peak observed at around –0.38 V, which is in a good agreement with the result of cyclic voltammogram test in Fig. 3. The asymmetry could be resulted from the overpotential caused by the reduction of Pb(II) to the liquid Pb metal. Resultantly, the increase of the current is delayed, and thus the increasing part of the current

is sharper than the decreasing one. A similar phenomenon has also been reported in electrochemical deposition of liquid metal tin in eutectic LiCl–KCl melts [31]. Accordingly, the disturbance of the signal due to the formation of liquid metal could be resolved by only taking the decreasing part of the peak into account for the measurement of the width of the half peak ($W_{1/2}$). Based on this methodology, the value of $W_{1/2}$ is 0.16 V, as depicted by the red dotted curve in Fig. 4. In the case of a reversible system, the number of exchanged electrons n in the electrochemical process can then be determined according to Eq. (3) [32]. The value of n is calculated to be 1.85, close to 2.0. This reveals that the reduction of Pb(II) to Pb metal proceeds through a single step with two electrons exchanged. The result is consistent with that investigated by cyclic voltammogram.

$$W_{1/2} = \frac{3.52RT}{nF} \quad (3)$$

where R is the mole gas constant (8.314 J/(mol·K)), and T is the thermodynamic temperature (K).

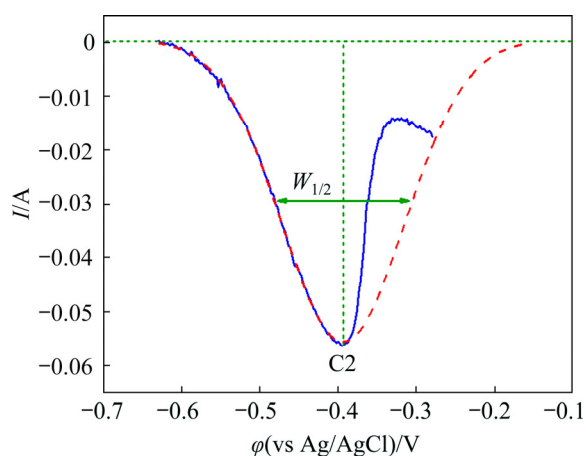


Fig. 4 Square wave voltammogram of Pb(II) measured on tungsten electrode in NaCl–KCl melts at 700 °C and frequency of 30 Hz

The reversibility of the redox reaction of Pb(II)/Pb(0) was then investigated over a wide scan rate range. As shown in Fig. 5, with the scan rate increasing from 0.10 to 0.70 V/s, the cathodic peak shifts towards negative potential while the anodic peak shifts towards positive potential slightly, indicating that the reduction reaction of Pb(II) to metallic Pb(0) is a quasi-reversible process. Meanwhile, it is indicated that the cathodic/anodic peak currents increase as the scan rate increases.

The correlation of the cathodic peak current (I_p) with the square root of scan rate was plotted and presented in Fig. 6. It exhibits good linear relationship, and suggests that the electrochemical reduction of Pb(II) in NaCl–KCl melts is a diffusion-controlled process. For a reversible soluble/insoluble system, the diffusion coefficient can be quantitatively determined by the Berzins–Delahay equation [33]:

$$I_p = -0.61SC_0(nF)^{3/2}D^{1/2}v^{1/2}(RT)^{-1/2} \quad (4)$$

where S is the electrode surface area (cm^2), C_0 denotes the solute concentration (mol/cm^3), D is the diffusion coefficient (cm^2/s), and v designates the potential scan rate (V/s). According to the slope of the straight line in Fig. 6, the diffusion coefficient of Pb(II) ions in NaCl–KCl melts at 700 °C is calculated to be $1.7 \times 10^{-5} \text{ cm}^2/\text{s}$ by assuming that $n=2$.

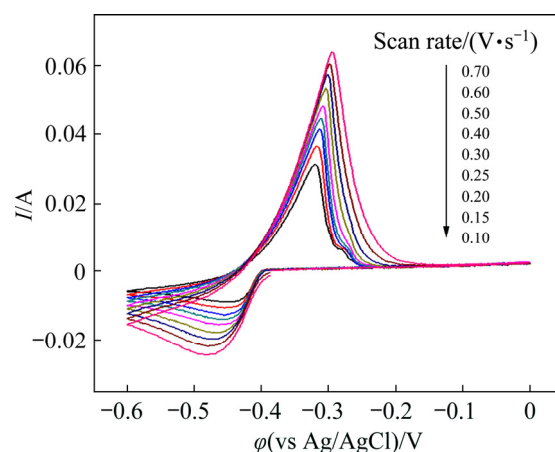


Fig. 5 Cyclic voltammograms of reduction of Pb(II) on tungsten electrode in NaCl–KCl–PbCl₂ melts at different scan rates

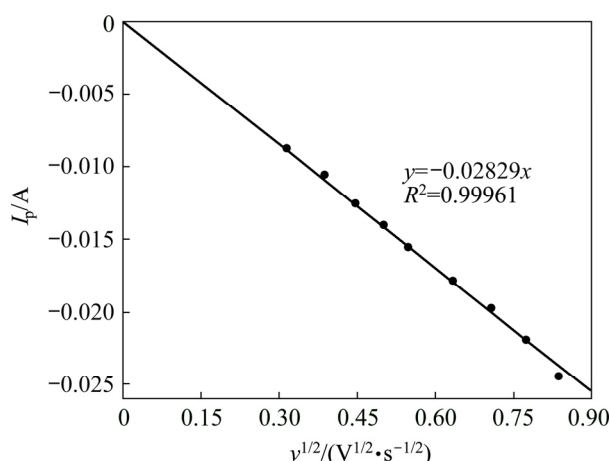


Fig. 6 Relationship between cathodic peak current and square root of scan rate in NaCl–KCl–PbCl₂ melts

It is worth mentioning that the CV curves at a scan rate from 0.10 to 0.30 V/s in Fig. 5 show a small anodic peak, which is insignificant compared with the main oxidation peak. Similar phenomena have also been observed by XIAO et al [29] and VANDARKUZHALI et al [34]. It was reported that this small peak could be attributed to the monolayer dissolution of the deposited product, and it was highly specific with respect to the electrode surface [34]. After serving for several cyclic voltammetry tests at low scan rates, the surface of the tungsten working electrode was probably affected by the deposited product. Therefore, the subsequent cyclic voltammograms at a scan rate from 0.40 to 0.70 V/s in Fig. 5 do not show any monolayer dissolution peak.

To further investigate the electrochemical behavior of Pb(II), linear sweep voltammograms were also recorded on tungsten working electrode in NaCl–KCl melts with various PbCl₂ concentrations. As shown in Fig. 7, the cathodic peak current increases distinctly with the increase of the PbCl₂ concentration, suggesting that more electricity is consumed and subsequently thicker deposit generated in the melts with higher concentration of the reactant, which is in conformity to fact that the cathodic peak current linearly depends on solute concentration according to the Berzins–Delahay equation [33,35]. Furthermore, the relationship between the electrode potential (φ) of the Pb²⁺/Pb redox reaction and PbCl₂ concentration can also be estimated according to the Nernst equation [32], as shown as follows:

$$\varphi = \varphi^0 + \frac{RT}{nF} \ln\left(\frac{\alpha_{\text{Pb(II)}}}{\alpha_{\text{Pb}}}\right) = \varphi^0 + \frac{RT}{nF} \ln\left(\frac{\gamma_{\text{Pb}^{2+}} c_{\text{Pb(II)}}}{\gamma_{\text{Pb}} c_{\text{Pb}}}\right) \quad (5)$$

where φ^0 is the standard redox potential (V), $\alpha_{\text{Pb(II)}}$ and α_{Pb} are the activities of Pb(II) and Pb, $\gamma_{\text{Pb(II)}}$ and γ_{Pb} are the activity coefficients of Pb(II) and Pb, and $c_{\text{Pb(II)}}$ and c_{Pb} are the concentrations of Pb(II) and Pb, respectively. Pb is insoluble in the molten system, and thus its activity can be regarded as the constant of 1. Therefore, the initial reduction potential shifts positively as the concentration of PbCl₂ increases, as demonstrated in Fig. 7. The initial reduction potential of Pb provides a theoretical basis for selecting an appropriate cell voltage during lead electrolysis.

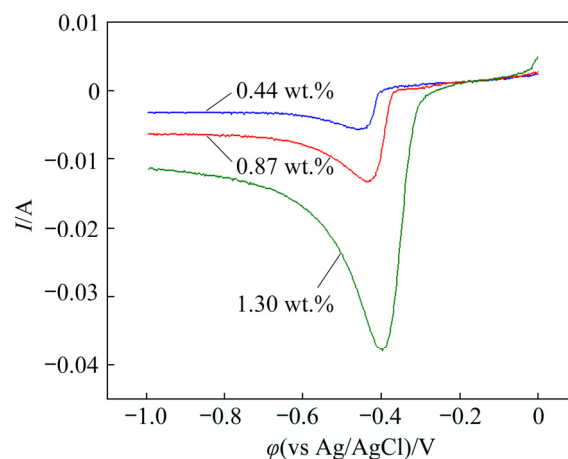


Fig. 7 Linear sweep voltammograms of Pb(II) on tungsten electrode in eutectic NaCl–KCl melts with different contents of PbCl₂ at 700 °C and scan rate of 0.10 V/s

Chronopotentiometry was also executed to further verify the electrochemical reduction process of Pb(II). Figure 8 presents the chronopotentiogram curves of Pb(II) obtained on tungsten electrode in NaCl–KCl–PbCl₂ melts with the applied current from –10 to –30 mA. The potential–time curves show two potential plateaus at around –0.4 and –2.0 V (vs Ag/AgCl), corresponding to the reduction of Pb(II) to Pb(0) and Na(I) to Na(0), respectively. These two plateaus are in the same potential range as that observed in cyclic voltammogram and square wave voltammogram. It can be seen that the negative shift of Plateau I is not evident and nearly independent of the applied current, further confirming that the reduction of Pb(II) to Pb(0) is controlled by the diffusion process. Herein, transition time (τ) stands for the necessary time to observe the complete depletion of Pb(II), originating from the layer of electrolyte around the electrode surface through diffusion, and it consequentially decreases as the applied current increases. The transition time was measured according to the method introduced in Ref. [36]. Additionally, the current shows a linear relationship with the reciprocal of the square root of the transition time, as shown in Fig. 9. Therefore, the following Sand equation is valid to estimate the diffusion coefficient of Pb(II):

$$I\tau^{1/2} = 0.5nFSC_0\pi^{1/2}D^{1/2} \quad (6)$$

It is also assumed that two electrons are transferred and the diffusion coefficient of Pb(II) in eutectic NaCl–KCl at 700 °C is $1.9 \times 10^{-5} \text{ cm}^2/\text{s}$

according to the slope of the straight line, which is very close to that acquired by the cyclic voltammogram.

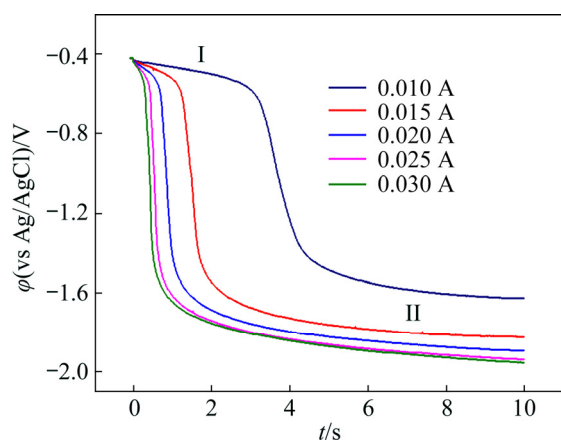


Fig. 8 Chronopotentiogram curves of Pb(II) on tungsten electrode ($S=0.322 \text{ cm}^2$) in NaCl–KCl–1.15wt.%PbCl₂ melts at 700 °C and different currents

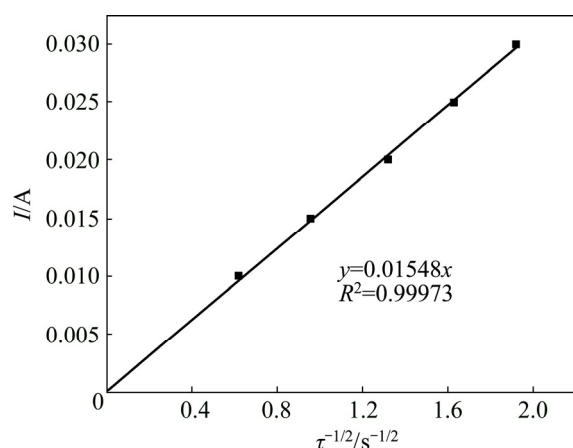


Fig. 9 Relationship between current and reciprocal square root of transition time

3.3 Electrochemical extraction and XRD pattern of lead metal

To verify the feasibility of electrochemically extracting lead metals, potentiostatic electrolysis was carried out at -0.6 V (vs Ag/AgCl) in molten NaCl–KCl–PbCl₂ at 700 °C on the tungsten electrode, according to the results obtained by cyclic voltammetry, linear sweep voltammetry, square wave voltammetry and chronopotentiometry. After electrolysis for 10 h, the bulk metal (see inset in Fig. 10) was obtained in the bottom of the melts beneath the tungsten cathode. Owing to the fairly low melting temperature, the metal generated on cathode during electrolysis would gradually grow into liquid droplets and then fall down to the bottom

of the crucible, and eventually solidify to spheroid granules during shutting down and cooling of the system. Figure 10 shows the XRD pattern of the cathodic product, and the observed characteristic peaks are identified as lead, definitely confirming that pure lead metal can be obtained through direct electrolysis of PbCl₂ in eutectic NaCl–KCl melts. Therefore, the mixture of NaCl–KCl salt with the eutectic composition is considered as a suitable supporting electrolyte for the electrochemical reduction of Pb(II) and for direct electrodeposition of Pb metal. This investigation lays a foundation to further study the efficient extraction of lead from spent LABs via the proposed salt extraction process. Of course, more technical and economical assessment of the process should still be further conducted in the future work to optimize the proposed route for achieving efficient recovery of lead from spent LABs.

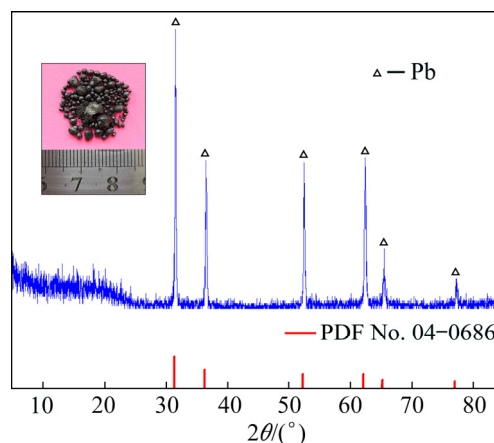


Fig. 10 XRD pattern of cathodic product (inset photo) obtained by potentiostatic electrolysis at -0.6 V (vs Ag/AgCl) in NaCl–KCl–PbCl₂ melts at 700 °C

4 Conclusions

(1) The thermodynamic calculation results indicate that the Pb-bearing phases of PbSO₄, PbO₂, PbO and Pb in the spent LABs could be converted to PbCl₂ by chlorination roasting, while PbCl₂ would be preferentially reduced to Pb metal due to its fairly low decomposition voltage via molten salt electrolysis. This confirms that the salt extraction process is an alternative and feasible route for the effective recovery of Pb from spent LABs.

(2) The electrochemical behavior of Pb(II) on a tungsten electrode was investigated in eutectic NaCl–KCl melts at 700 °C using cyclic

voltammetry, linear sweep voltammetry, square wave voltammetry and chronopotentiometry. Pb(II) can be directly reduced to Pb metal in NaCl–KCl melts through a single step with two electrons exchanged, and the initial reduction potential is approximately -0.38 V (vs Ag/AgCl). Meanwhile, the reduction process is quasi-reversible and controlled by diffusion, and the diffusion coefficient of Pb(II) in the melts was determined to be 1.7×10^{-5} and 1.9×10^{-5} cm^2/s according to the results of cyclic voltammetry and chronopotentiometry using the Berzins–Delahay equation and the Sand equation, respectively.

(3) Potentiostatic electrolysis was performed at -0.6 V (vs Ag/AgCl) in NaCl–KCl–PbCl₂ melts at 700 °C and spheroidic bulk metals were obtained. The cathodic products were confirmed to be pure Pb by XRD analysis. The results of this work demonstrate that pure lead metal can be produced by direct electrolysis of PbCl₂ in eutectic NaCl–KCl melts at 700 °C, and the feasibility of recycling lead from spent LABs via salt extraction process is further verified.

References

- [1] ZHANG Wei, YANG Jia-kuan, WU Xu, HU Yu-chen, YU Wen-hao, WANG Jun-xiong, DONG Jin-xin, LI Ming-yang, LIANG Sha, HU Jing-ping, KUMAR R V. A critical review on secondary lead recycling technology and its prospect [J]. Renewable and Sustainable Energy Reviews, 2016, 61: 108–122.
- [2] ZHANG Mi-lin, CHEN Li-jun, HAN Wei, YAN Yong-de, CAO Peng. Electrochemical behavior of Pb(II) in LiCl–KCl–MgCl₂–PbCl₂ melts on Mo electrode [J]. Transactions of Nonferrous Metals Society of China, 2012, 22: 711–716.
- [3] GUPT Y, SAHAY S. Managing used lead acid batteries in India: Evaluation of EPR-DRS approaches [J]. Journal of Health & Pollution, 2015, 5: 52–63.
- [4] ELLIS T W, MIRZA A H. The refining of secondary lead for use in advanced lead-acid batteries [J]. Journal of Power Sources, 2010, 195: 4525–4529.
- [5] SUN Zhi, CAO Hong-bin, ZHANG Xi-hua, LIN Xiao, ZHENG Wen-wen, CAO Guo-qiang, SUN Yong, ZHANG Yi. Spent lead-acid battery recycling in China—A review and sustainable analyses on mass flow of lead [J]. Waste Management, 2017, 64: 190–201.
- [6] LI L, ZHU X F, YANG D N, GAO L X, LIU J W, KUMAR R V, YANG J K. Preparation and characterization of nano-structured lead oxide from spent lead acid battery paste [J]. Journal of Hazardous Materials, 2012, 203: 274–282.
- [7] HU Biao, YANG Fan, CHEN Long. Research progress of technology for recycling lead paste from spent lead-acid batteries [J]. Applied Chemical Industry, 2019, 48: 2742–2748. (in Chinese)
- [8] JIANG Ji-mu. Situation and development trend of lead smelting technology at home and abroad [J]. Energy Saving of Nonferrous Metallurgy, 2013, 3: 4–8. (in Chinese)
- [9] CHEN Lai-guo, XU Zhen-cheng, LIU Ming, HUANG Yu-mei, FAN Rui-fang, SU Yan-hua, HU Guo-cheng, PENG Xiao-wu, PENG Xiao-chun. Lead exposure assessment from study near a lead-acid battery factory in China [J]. Science of the Total Environment, 2012, 429: 191–198.
- [10] WANG Hong-jun, FENG Ya-li, LI Hao-ran, KANG Jin-xing. Simultaneous extraction of gold and zinc from refractory carbonaceous gold ore by chlorination roasting process [J]. Transactions of Nonferrous Metals Society of China, 2020, 30: 1111–1123.
- [11] HUA Zhong-sheng, GENG Ao, TANG Ze-tao, ZHAO Zhuo, LIU Huan, YAO Yong-lin, YANG Yong-xiang. Decomposition behavior and reaction mechanism of Ce_{0.67}Tb_{0.33}MgAl₁₁O₁₉ during Na₂CO₃ assisted roasting: Toward efficient recycling of Ce and Tb from waste phosphor [J]. Journal of Environmental Management, 2019, 49: 109383.
- [12] LI Jin-hui, LI Yang-yang, GAO Yan, ZHANG Yun-fang, CHEN Zhi-feng. Chlorination roasting of laterite using salt chloride [J]. International Journal of Mineral Processing, 2016, 148: 23–31.
- [13] LI H Y, MA A Y, SRINIVASAKANNAN C, ZHANG L B, LI S W, YIN S H. Investigation on the recovery of gold and silver from cyanide tailings using chlorination roasting process [J]. Journal of Alloys and Compounds, 2018, 763: 241–249.
- [14] YANG Cong-cong, ZHU De-qing, PAN Jian, LI Si-wei, TIAN Hong-yu. A novel process for Fe recovery and Zn, Pb removal from a low-grade pyrite cinder with high Zn and Pb contents [J]. International Journal of Minerals, Metallurgy and Materials, 2018, 25: 981–989.
- [15] ABBASALIZADEH A, SEETHARAMAN S, TENG L, SRIDHAR S, GRINDER O, IZUMI Y, BARATI M. Highlights of the salt extraction process [J]. JOM, 2013, 65: 1552–1558.
- [16] LIU Zhen-wei, ZHANG Hong-ling, PEI Li-li, SHI Yi-lang, CAI Zhi-hua, XU Hong-bin, ZHANG Yi. Direct electrolytic preparation of chromium metal in CaCl₂–NaCl eutectic salt [J]. Transactions of Nonferrous Metals Society of China, 2018, 28: 376–384.
- [17] WANG Yin-shuai, ZOU Xing-li, LU Xiong-gang, LI Shang-shu, ZHENG Kai, WANG Shu-juan, XU Qian, ZHOU Zhong-fu. Electrolytic production of Ti–Ge intermetallics from oxides in molten CaCl₂–NaCl [J]. Transactions of Nonferrous Metals Society of China, 2018, 28: 2351–2359.
- [18] HUA Zhong-sheng, WANG Jian, WANG Lei, ZHAO Zhuo, LI Xin-lei, XIAO Yan-ping, YANG Yong-xiang. Selective extraction of rare earth elements from NdFeB scrap by molten chlorides [J]. ACS Sustainable Chemistry & Engineering, 2014, 2: 2536–2543.
- [19] PERSHIN P, KHALIMULLINA Y, ARKHIPOV P, ZAIKOV Y. The electrodeposition of lead in LiCl–KCl–PbCl₂ and LiCl–KCl–PbCl₂–PbO melts [J]. Journal of The Electrochemical Society, 2014, 161: 824–830.
- [20] ARKHIPOV P A, KHOLKINA A S, ZAYKOV Y P, ARKHIPOV S P. Anode dissolution of ternary Pb–Sb–Bi alloys and reduction of lead in the KCl–PbCl₂ melt [J]. Journal of the Iranian Chemical Society, 2019, 16: 2501–2507.

- [21] HAN Wei, WANG Wen-juan, DONG Yong-chang, LI Mei, YANG Xiao-guang, ZHANG Mi-lin. The kinetics process of a Pb(II)/Pb(0) couple and selective fabrication of Li–Pb alloys in LiCl–KCl melts [J]. RSC Advances, 2018, 8: 30530–30538.
- [22] HUA Zhong-sheng, LIU Huan, WANG Jian, HE Ji-wen, XIAO Sai-jun, XIAO Yan-ping, YANG Yong-xiang. Electrochemical behavior of neodymium and formation of Mg–Nd alloys in molten chlorides [J]. ACS Sustainable Chemistry & Engineering, 2017, 5: 8089–8096.
- [23] HE Ji-wen, HUA Zhong-sheng, LIU Huan, XU Liang, HE Shi-wei, YANG Yong-xiang, ZHAO Zhuo. Redox behavior of yttrium and electrochemical formation of Y–Al alloys in molten chlorides [J]. Journal of the Electrochemical Society, 2018, 165: 598–603.
- [24] XU Cong, CHENG Hong-wei, LI Guang-shi, LU Chang-yuan, LU Xiong-gang, ZOU Xing-li, XU Qian. Extraction of metals from complex sulfide nickel concentrates by low-temperature chlorination roasting and water leaching [J]. International Journal of Minerals Metallurgy and Materials, 2017, 24: 377–385.
- [25] YANG Zhong-yu. Metallurgy of light metals [M]. Beijing: Metallurgical Industry Press, 2013. (in Chinese)
- [26] CAI Zhuo-fei, GUO Zhan-cheng, TANG Hui-qing, ZHANG Zhi-mei. Application of KCl–NaCl–CaCl₂ ternary molten salts in FFC Cambridge process [J]. Journal of Rare Earths, 2011, 29: 8–13. (in Chinese)
- [27] FU Chong-shuo. Theory of nonferrous metallurgy [M]. 2nd ed. Beijing: Metallurgical Industry Press, 2010. (in Chinese)
- [28] LIU Kang, YANG Jia-kuang, LIANG Sha, HOU Hui-jie, CHEN Ye, WANG Jun-xiong, LIU Bing-chuan, XIAO Ke-ke, HU Jing-ping, WANG Jin. An emission-free vacuum chlorinating process for simultaneous sulfur fixation and lead recovery from spent lead-acid batteries [J]. Environmental Science & Technology, 2018, 52: 2235–2241. (in Chinese)
- [29] XIAO Sai-jun, LIU Wei, GAO Long. Cathodic process of manganese (II) in NaCl–KCl melt [J]. Ionics, 2016, 22: 2387–2390.
- [30] ZHANG Zheng, SONG Qiu-shi, JIANG Bao-cheng, XIE Hong-wei, YIN Hua-yi, NING Zhi-qiang, XU Qian. Electrochemically assisted carbonization of Nb in molten salt [J]. Surface and Coating Technology, 2019, 358: 865–872.
- [31] CAI Yan-qing, CHEN Xing-gang, XU Qian, XU Ying. Electrochemical behaviour of tin in a LiCl–KCl eutectic melt [J]. International Journal of Electrochemical Science, 2018, 13: 10786–10797.
- [32] BARD A J, FAULKNER L R. Electrochemical methods: Fundamentals and applications [M]. New York: John Wiley & Sons, 2001.
- [33] BERZINS T, DELAHAY P. Oscillographic polarographic waves for the reversible deposition of metals on solid electrodes [J]. Journal of the American Chemical Society, 1953, 75: 555–559.
- [34] VANDARKUZHALI S, VENKATESH P, GHOSH S, SEENIVASAN G, REDDY B P, SUBRAMANIAN T, SIVARAMAN N, NAGARAJAN K. Electrochemistry of rare earth oxy ions REO⁺ (RE=Ce, La, Nd) in molten MgCl₂–NaCl–KCl eutectic [J]. Journal of Electroanalytical Chemistry, 2007, 611: 181–191.
- [35] KIM D H, BAE S E, PARK T H, KIM J Y, LEE C W, SONG K. Real-time monitoring of metal ion concentration in LiCl–KCl melt using electrochemical techniques [J]. Microchemical Journal, 2014, 114: 261–265.
- [36] LAITY R W, MCINTYRE J D E. Chronopotentiometric diffusion coefficients in fused salts I: Theory [J]. Journal of the American Chemical Society, 1965, 87: 3806–3812.

NaCl–KCl 共融盐中铅的电化学行为与电解制备

朱曾丽¹, 刘欢^{1,2}, 陈杰双阳¹, 孔辉^{1,3}, 徐亮¹, 华中胜^{1,3}, 赵卓¹

1. 安徽工业大学 冶金工程学院, 马鞍山 243032;

2. 铜陵有色金属集团控股有限公司 金冠铜业分公司, 铜陵 244000;

3. 安徽工业大学 冶金工程与资源综合利用安徽省重点实验室, 马鞍山 243002

摘要: 为了开发高效、环境友好的废铅酸电池回收工艺, 提出一种基于氯化焙烧和熔盐电解的新型处理方法。首先, 通过热力学分析对熔盐法从废铅酸电池中回收铅的可行性进行论证。然后, 采用电化学暂态测试方法对 700 °C 时 NaCl–KCl 共融盐中 Pb(II) 在钨电极上的电化学行为进行深入研究。结果表明: Pb(II) 在 NaCl–KCl 熔盐中的还原反应是一步交换 2 个电子的准可逆过程, 且该过程受准可逆扩散控制。最后, 于 –0.6 V (vs Ag/AgCl) 电位下在 NaCl–KCl–PbCl₂ 熔盐中进行恒电位电解, 所得阴极产物经 X 射线衍射分析证实为纯 Pb。本研究表明, 在 NaCl–KCl 共融盐中电解还原 PbCl₂ 制备金属铅是切实可行的, 并为熔盐法从废铅酸电池中回收铅的后续研究提供重要理论依据。

关键词: 电化学行为; Pb(II); 还原; 废铅酸电池; NaCl–KCl 共融盐

(Edited by Wei-ping CHEN)